The Response and Failure of Local Sharp-cut 6061-T6 Aluminum Alloy Tubes with Different Diameter-to-thickness Ratios Submitted to Cyclic Bending

Kuo-Long Lee [1*], Wei-Yi Huang [2], Wen-Fung Pan [3]

[1] Department of Innovative Design and Entrepreneurship Management, Far East University
[2-3] Department of Engineering Science, National Cheng Kung University

ABSTRACT

In this paper, the response and failure of local sharp-cut 6061-T6 aluminum alloy tubes with different diameter-to-thickness ratios submitted to cyclic bending were studied. Three different diameter-to-thickness ratios of 16.5, 31.0 and 60.0 were considered. The experimental moment-curvature relationship rapidly became a steady loop from the beginning of the first bending cycle. Moreover, the cut depth had almost no influence on the moment-curvature relationship. As for the ovalization-curvature relationship, when the number of cycles increased, it exhibited an increasing and ratcheting manner. It was seen that the greater the depth of the cut, the more asymmetrical ovalization-curvature relationship and the greater the increase of the ovalization. Furthermore, for a certain diameter-to-thickness ratio, five unparallel straight lines corresponding to five different cut depths were found for the controlled curvature-number of cycles required to produce failure relationship on a log-log scale. Finally, a theoretical model was proposed in this study for simulating aforementioned relationship. It was found that the experimental and analytical data agreed well.

Key words: Local Sharp-cut, 6061-T6 Aluminum Alloy Tubes, Diameter-to-thickness Ratio, Cyclic Bending, Response, Failure.

不同外徑/壁厚比局部切痕 6061-T6 鋁合金圓管在循環彎曲負載下行為與損壞之研究

李國龍 [1*]　黃文義 [2]　潘文峰 [3]

[1] 遠東科技大學創新設計與創業管理系
[2-3] 國立成功大學工程科學系

摘　要

本文主要是研究不同外徑/壁厚比的局部尖銳切痕 6061-T6 鋁合金圓管在循環彎曲負載下的行為及損壞，而所考慮的三種不同外徑/壁厚比包含有：16.5、31.0 及 60.0。從實驗的彎矩-曲率曲線中顯示，彎矩-曲率關係從第一圈開始即快速呈現一穩定的迴圈，且切痕深度對彎矩-曲率關係幾乎沒有影響。至於橢圓化-曲率關係則隨著循環圈數的增加而呈現棘齒狀的成長，且切痕深度

Lee et al.
The Response and Failure of Local Sharp-cut Circular Tubes with Different Diameter-to-thickness Ratios Submitted to
Cyclic Bending

越深時，橢圓化-曲率關係就越不對稱，橢圓化增加就越大。此外，當考慮個別外徑/壁厚比時，五種不同切痕深度在雙對數座標的控制曲率-循環至損壞圈數關係呈現出五條不平行的直線。最後，本研究提出一個理論模式來描述控制曲率-循環至損壞圈數關係，在與實驗結果比較後發現，理論能夠合理描述實驗結果。

關鍵詞：局部尖銳切痕、6061-T6 鋁合金管、外徑/壁厚比、循環彎曲、反應、損壞。

I. INTRODUCTION

Circular tubes are often used in mechanical or structural components, for example earthquake-prone-area structures, drilling oil platform, subsea pipelines, and heat exchangers in power plants or nuclear reactors. However, these tube components are frequently submitted to bending load, which brings about the ovalization of tube's cross section. And reverse and continuous cyclic bending leads to gradual increase in ovalization. The ovalization phenomenon leads to the degradation of the tube's rigidity. The circular tube failures (buckling or fracture) when the ovalization reaches a crucial value. Therefore, it is of importance to completely understand the response during the cyclic bending process and failure at the final stage of circular tubes submitted to cyclic bending in many industrial applications.

In 1985, Prof. Kyriakides and his research team designed a bending machine and began a series of experimental and theoretical studies on tubes submitted to monotonic or cyclic bending with or without external or internal pressure. Shaw and Kyriakides [1] studied the elastoplastic behavior of tubes under cyclic bending. The moment-curvature and ovalization-curvature relationships were theoretically simulated using the principle of virtual work. Kyriakides and Shaw [2] then extended the aforementioned research to evaluate the buckling failure of tubes under cyclic bending. They suggested an empirical form to describe the controlled curvature and the number of cycles required to produce a buckling relationship. Meanwhile, Corona and Kyriakides [3] experimentally investigated the behavior of tubes subjected to cyclic bending with some external pressure. They discovered that the accumulation of ovalization was accelerated by applying some external pressure. Vaze and Corona [4]

employed a similar bending machine to examine the deterioration and collapse of square steel tubes submitted to cyclic bending. They discovered that the tubes deteriorated because of the growth of periodic deflections in the flanges. Moreover, Corona and Kyriakides [5] studied the tube's buckling under bending with some external pressure. In their work, 304 stainless steel tubes exhibited the angle buckling oriented at 20-45° to the direction of the bending moment. Similarly, Corona et al. [6] investigated the anisotropy of the plastic deformation for tubes submitted to bending. The material anisotropy behavior at the pre-buckling, post-buckling, and bifurcation stages was simulated by flow and deformation theories. Limam et al. [7] experimentally and theoretically discussed the inelastic collapse of tubes subjected to bending with some internal pressure. They employed the shell model in the finite element method to evaluate tube wrinkling and localization. Limam et al. [8] also examined the response and collapse of local-dented tubes undertaking pure bending with some internal pressure. The dent processing, tube pressurization, and tube bending to collapse were described through the finite element method. Bechle and Kyriakides [9] experimentally investigated the localization of NiTi tubes submitted to bending. In addition, the influence of the texture-driven and material asymmetry on the tube structure was studied. Jiang et al. [10] studied the pseudooelastic response of NiTi tubes subjected to bending. A recently developed constitutive model for the pseudoelastic behavior was implemented in a finite element analysis used to simulate the tube bending experiments.

Other researchers have also published numerous related studies. Yuan and Mirmiran [11] experimentally and theoretically investigated the static buckling of fiber-reinforced plastic tubes filled with concrete subjected to bending. Elchalakani et al. [12]

experimentally tested on grade C350 steel tubes with different diameter-to-thickness ratios (D_o/t ratios) submitted to pure bending. They proposed two theoretical models to simulate the experimental results. Meanwhile, Jiao and Zhao [13] experimentally investigated the bending behavior of very high-strength steel tubes and proposed a plastic slenderness limit for the material they tested. Moreover, Houliara and Karamanos [14] investigated the elastic response of long-pressurized, thin-walled tubes at the buckling and post-buckling stages undertaken in-phase bending. Elchalakani and Zhao [15] focused on concrete-filled and cold-formed steel tubes subjected to monotonic and cyclic bending with variable amplitudes. Yazdani and Nayebi [16] investigated the response and damage of thin-walled tubes submitted to cyclic bending with a steady internal pressure. Fan *et al.* [17] presented an analytical study on the critical dynamic buckling load of cylindrical shells under a uniform external pressure. Elchalakani *et al.* [18] determined new ductile slenderness limits of CFT structures during plastic design using measured strains in plastic bending tests. Shamass *et al.* [19] investigated the elastoplastic buckling of thin circular shells subjected to a non-proportional loading.

In 1998, Pan *et al.* [20] designed and set up a new measurement apparatus. The apparatus was used with a cyclic bending machine to study various types of tube under different cyclic bending conditions. For examples: Pan and Fan [21] studied the effect of the prior curvature-rate at the preloading stage on subsequent creep or relaxation behavior, Pan and Her [22] investigated the response and stability of 304 stainless steel tubes that were subjected to cyclic bending with different curvature rates, Lee *et al.* [23] studied the influence of the D_o/t ratio on the response and stability of circular tubes that were subjected to symmetrical cyclic bending, Lee *et al.* [24] experimentally explored the effect of the D_o/t ratio and curvature-rate on the response and stability of circular tubes subjected to cyclic bending, Chang *et al.* [25] studied the mean moment effect on circular, thin-walled tubes under cyclic bending, and Chang and Pan [26] discussed the buckling life estimation of

circular tubes subjected to cyclic bending.

In 2010, the research team of Prof. Pan began to experimentally and theoretically investigate the response and the collapse of sharp-notched circular tubes submitted to cyclic bending. Lee *et al.* [27] experimentally studied the relationship between the variation of ovalization and the number of bending cycles for sharp-notched circular tubes subjected to cyclic bending. Lee [28] investigated the response of sharp-notched SUS304 stainless steel tubes under cyclic bending, and found the asymmetrical, ratcheting, and increasing trends of ovalization-curvature relationships. Hung *et al.* [29] then later experimental investigated on the mechanical response and buckling failure of SUS304 stainless steel tubes with five different sharp-notched depths subjected to cyclic bending with three different curvature rates. In addition, Lee *et al.* [30] evaluated the viscoplastic response and buckling of sharp-notched SUS304 stainless steel circular tubes undertaking cyclic bending. They observed that the cyclic controlled curvature and the number of bending cycles required to produce buckling relationships on a log-log scale revealed parallel lines for every notch depths for a certain curvature rate. Lee *et al.* [31] studied the response of sharp-notched circular tubes under pure bending creep. They found that the creep curvature and ovalization increase with time for pure bending creep and higher held moment leads to the higher creep curvature and ovalization of the tube's cross-section. However, the sharp notch for the aforementioned investigations was a circumferential sharp notch as shown in Fig. 1.
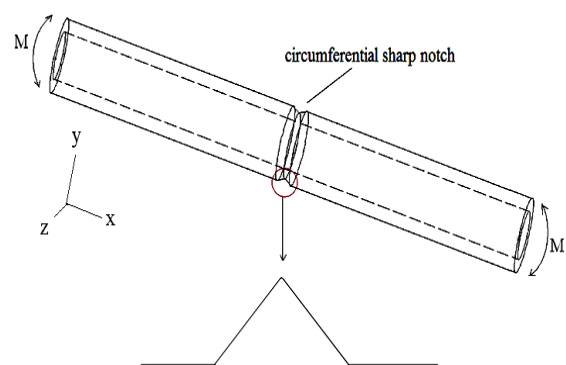

Fig. 1 A schematic drawing of the circumferential sharp-notched tube

Lee et al.
The Response and Failure of Local Sharp-cut Circular Tubes with Different Diameter-to-thickness Ratios Submitted to
Cyclic Bending

The investigation of the influence of the D_o/t ratio on the response and failure was first investigated by Lee *et al.* [23]. The 304 stainless steel smooth tubes with four different D_o/t ratios of 30, 40, 50 and 60 were tested under cyclic bending. Later, Chang *et al.* [32] studied the buckling failure of 301 stainless steel smooth tubes with different D_o/t ratios subjected to cyclic bending. In 2012, Lee *et al.* [33] started to investigate the influence of the D_o/t ratio on the response and failure of sharp-notched 304 stainless tubes under cyclic bending. The type of the sharp notch was in Fig. 1 and three different D_o/t ratios were 16.25, 21.20 and 24.46. They discover that five almost parallel straight lines corresponding to five different notch depths for each D_o/t ratio were observed from the controlled curvature and number of bending cycles required to produce failure relationship on a log-log scale. In addition, the slopes for the aforementioned relationship for three different D_o/t ratios were almost the same.

In this paper, local sharp-cut 6061-T6 aluminum alloy tubes with different D_o/t ratios of 16.5, 31.0 and 60.0 submitted to cyclic bending were experimentally studied. Related experimental tests were conducted by using the tube-bending machine and curvature-ovalization measurement apparatus. The quantities of bending moment, curvature and ovalization were measured by sensors on testing facilities. Additionally, the number of bending cycles required to produce failure was also recorded.

II. EXPERIMENTS

A tube-bending machine and a curvature-ovalization measurement apparatus were employed to conduct the cyclic bending test on local sharp-cut circular tubes with different D_o/t ratios. The details on the experimental device, materials, specimens, and test procedures were presented in the sections that follow.

Experimental Device

Fig. 2 schematically shows the experiments executed by a specially built tube-bending machine. This facility was set up to conduct monotonic, reverse, and cyclic bending tests. A detailed explanation of the experimental facility can be found in many papers (Pan *et al.* [20], Pan and Fan [21], Pan and Her [22], Lee *et al.* [23]). Pan *et al.* [20] designed a new light-weight apparatus to measure the curvature and the ovalization of the tube cross section as shown in Fig. 3. Two side-inclinometers in the apparatus were used to detect the tube's angle variation during cyclic bending. The tube curvature can be determined by a simple calculation according to the angle changes. An extended version of the calculation can be found in the work by Pan *et al.* [20]. In addition, the tube ovalization can be measured in the center part of the apparatus that included a magnetic detector and a magnetic block.
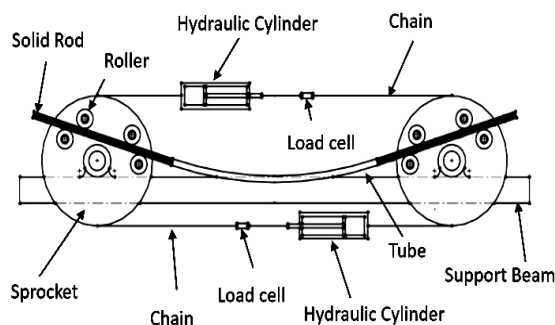

Fig. 2 A schematic drawing of the tube bending machine

Material and Specimens

6061-T6 aluminum alloy tubes were used for the experimental testing. Table 1 depicts the chemical composition (weight %) of the tested material. The mechanical properties were 0.2% offset yield stress (σ_o) = 166 MPa, ultimate stress (σ_u) = 258 MPa, and percent elongation = 23 %.
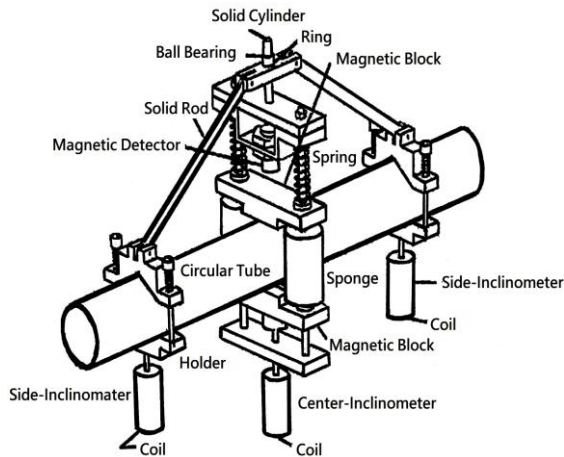
Fig. 3 A schematic drawing of the curvature-ovalization measurement apparatus

Table 1 Chemical composition of 6061-T6 aluminum alloy (weight %)

Chemical Composition	Al	Mg	Si	Cu	Ti	Fe
Proportion (%)	97.40	0.916	0.733	0.293	0.268	0.256
Chemical Composition	Mn	Zn	Cr	Ni	Pb	Sn
Proportion (%)	0.132	0.098	0.068	0.006	0.005	<0.001

The raw, unnotched 6061-T6 aluminum alloy circular tubes had a length L_o of 800 mm, an outside diameter D_o of 35.0 mm and a wall thickness t of 3.0 mm. The raw tubes were machined on the outside surface to obtain the desired D_o/t ratios of 16.5, 31.0 and 60.0 as shown in Fig. 4. However, the inner radiuses of all tested tubes were intact (29.0 mm).
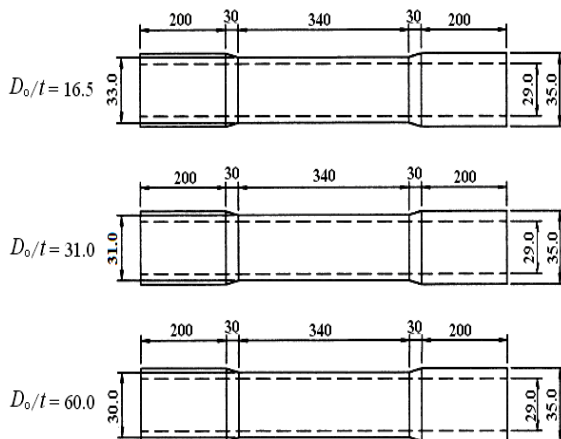
Fig. 4 A schematic drawing of tube's dimensions for D_o/t ratios of 16.5, 31.0 and 60.0

Next, tubes with a certain D_o/t ratio were

processed on the outside surface again to obtain the desired shape and depth of the cut. Fig. 5 shows a schematic drawing of the local sharp-cut circular tube, where the cut depth is denoted as a and the cut length is denoted as L_a. The relationship between a and L_a was determined by Lee *et al.* [34]. In this study, five different depth-to-thickness (a/t) ratios were considered: 0.0, 0.15, 0.3, 0.45, and 0.6. Note that $a/t = 0.0$ represents a tube with a smooth surface. It can be seen from Fig. 4 that the values of t for D_o/t ratios of 16.5, 31.0 and 60.0 are 2.0, 1.0 and 0.5 mm, respectively. Therefore, the magnitudes of a for $D_o/t = 16.5$, 31.0 and 60.0 are shown in Table 2. Fig. 6 shows a picture a local sharp-cut 6061-T6 aluminum alloy tube with $D_o/t = 16.5$ and $a = 0.0$, 0.3, 0.6, 0.9 and 1.2 mm. In addition, according to our measurement of a before the test, the error was within 10%.

Table 2 Magnitudes of a for $D_o/t = 16.5$, 31.0 and 60.0 (unit: mm)

D_o/t	a	a	a	a	a
16.5	0.0	0.3	0.6	0.9	1.2
31.0	0.0	0.15	0.3	0.45	0.6
60.0	0.0	0.075	0.15	0.225	0.3

Fig. 5 A schematic drawing of the local sharp-cut circular tube

Lee et al.
The Response and Failure of Local Sharp-cut Circular Tubes with Different Diameter-to-thickness Ratios Submitted to
Cyclic Bending
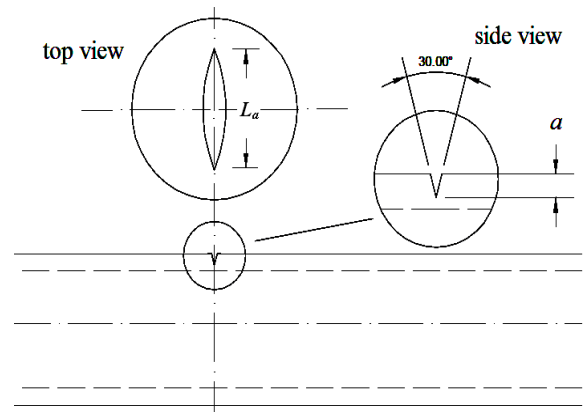
Fig. 6 A picture a local sharp-cut 6061-T6
aluminum alloy tube with $D_o/t = 16.5$ and
$a = 0.0, 0.3, 0.6, 0.9$ and 1.2 mm

Test Procedures

The test involved a curvature-controlled cyclic bending. The controlled-curvature ranges were from ± 0.2 to ± 1.1 m^{-1}, and the curvature rate of the cyclic bending test was 0.035 m^{-1}s^{-1}. The magnitude of the bending moment was measured by two load cells mounted to the bending device. The magnitude of the curvature and ovalization of the tube cross-section were controlled and measured by the curvature-ovalization measurement apparatus. In addition, the number of cycles required to produce failure was recorded. The timing of failure was the magnitude of the bending moment dropped 20%.

III. EXPERIMENT RESULTS AND DISCUSSION

Mechanical Behavior

Fig. 7 shows a typical set of experimentally determined cyclic moment (M) - curvature (κ) curves for a local sharp-cut 6061-T6 aluminum alloy circular tube, with $D_o/t = 16.5$ and $a = 1.2$ mm, subjected to cyclic bending. The tubes were cycled between $\kappa = \pm 0.3$ m^{-1}. It was observed that the M-κ relationship was linear for a small curvature. However, it became nonlinear for a large curvature. In addition, the M-κ response was seen to be characterized by a nearly closed and steady hysteresis loop from the first bending cycle. Since the sharp cut is small and local, the cut depth has almost no influence on the M-κ

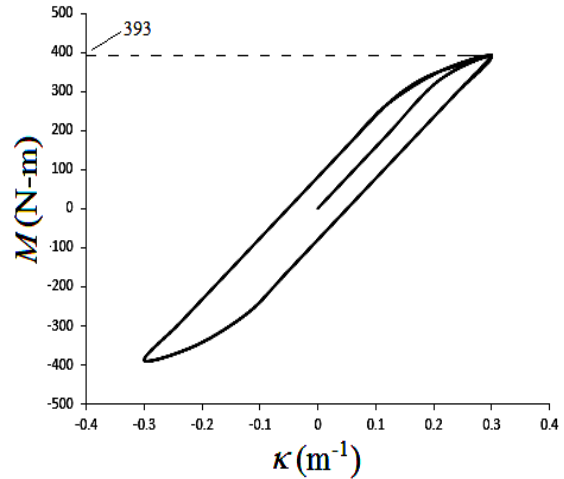curve. Therefore, the M-κ curves for $D_o/t = 16.5$ and different a are not shown in this paper.

Fig. 7 Experimental moment (M) - curvature (κ) curve for a local sharp-cut 6061-T6 aluminum alloy tube with $D_o/t = 16.5$ and $a = 1.2$ mm under cyclic bending

Figs. 8 and 9 demonstrate typical sets of experimentally determined cyclic moment (M) - curvature (κ) curves for local sharp-cut 6061-T6 aluminum alloy circular tubes, with $D_o/t = 31.0$, $a = 0.6$ mm and $D_o/t = 60.0$, $a = 0.3$ mm, respectively, subjected to cyclic bending. The tubes were cycled between $\kappa = \pm 0.3$ m^{-1}. Similar phenomenon of the M-κ curves with Fig. 7 was found. Because the thicknesses for $D_o/t = 31.0$ and 60.0 are smaller, so the bending moments at the $\kappa = +0.3$ m^{-1} are smaller. Again, the sharp cut is small and local, the cut depth has almost no influence on the M-κ curve. Therefore, the M-κ curves for $D_o/t = 31.0$ and 60.0 and different a are not shown in this paper.
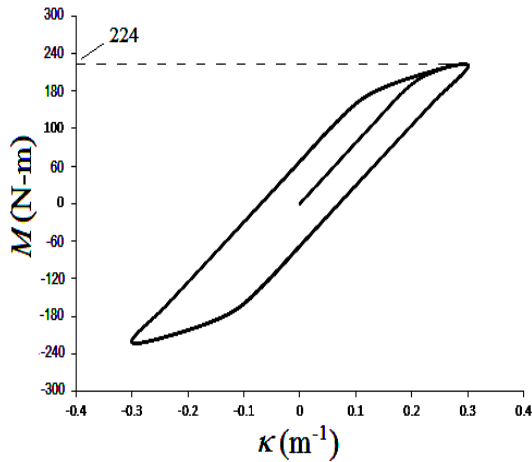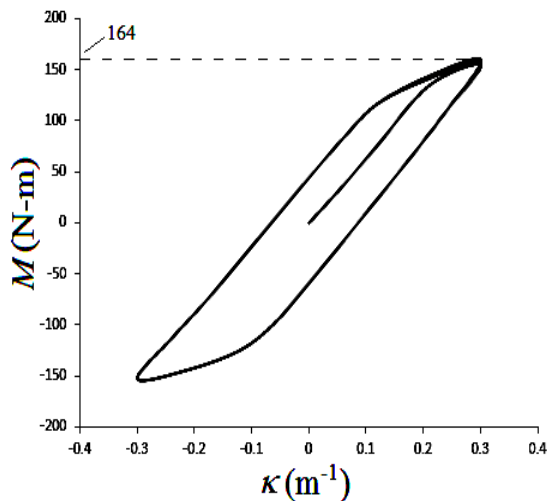
Fig. 8 Experimental moment (M) - curvature (κ) curve for a local sharp-cut 6061-T6 aluminum alloy tube with $D_o/t = 31.0$ and $a = 0.6$ mm under cyclic bending

Fig. 9 Experimental moment (M) - curvature (κ) curve for a local sharp-cut 6061-T6 aluminum alloy tube with $D_o/t = 60.0$ and $a = 0.3$ mm under cyclic bending

Figs. 10(a)-(e) depict the experimental relationships between the ovalization ($\Delta D_o/D_o$) and curvature (κ) for local sharp-cut 6061-T6 aluminum alloy tubes with $D_o/t = 16.5$ and $a = 0.0, 0.3, 0.6, 0.9,$ and 1.2 mm, respectively, under cyclic bending. The quantity of ΔD_o is the change in the outer diameter. The $\Delta D_o/D_o$-κ relationships exhibited a ratcheting and an increasing trend with the number of bending cycles. A larger a led to a more asymmetrical appearance of the $\Delta D_o/D_o$-κ relationship. Moreover, a larger a of the cut tubes caused a larger ovalization.
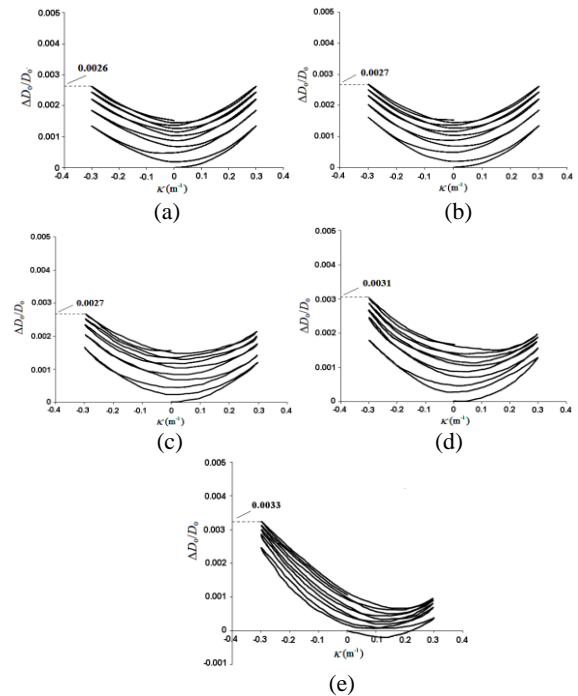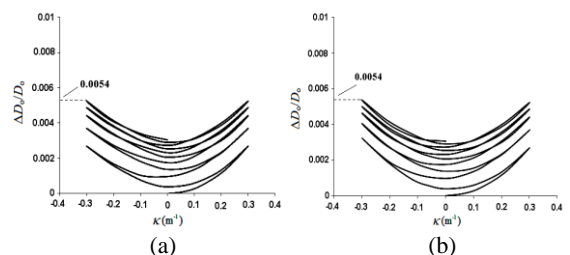

Fig. 10 Experimental ovalization ($\Delta D_o/D_o$) - curvature (κ) curves for local sharp-cut 6061-T6 aluminum alloy tubes with $D_o/t = 16.5$ and $a =$ (a) 0.0, (b) 0.3, (c) 0.6, (d) 0.9 and (e) 1.2 mm under cyclic bending

Figs. 11(a)-(e) depict the experimental relationships between the ovalization ($\Delta D_o/D_o$) and the curvature (κ) for local sharp-cut 6061-T6 aluminum alloy tubes with $D_o/t = 31.0$ and $a = 0.0, 0.15, 0.3, 0.45,$ and 0.6 mm respectively, under cyclic bending. Figs. 12(a)-(e) demonstrate the experimental relationships between the ovalization ($\Delta D_o/D_o$) and the curvature (κ) for local sharp-cut 6061-T6 aluminum alloy tubes with $D_o/t = 60.0$ and $a = 0.0, 0.075, 0.15, 0.225,$ and 0.3 mm, respectively, under cyclic bending. Similar phenomena with local sharp-cut 6061-T6 aluminum alloy tubes with $D_o/t = 16.5$ were found. In addition, a larger D_o/t ratio has a smaller wall thickness, thus, the ovalization increases faster.
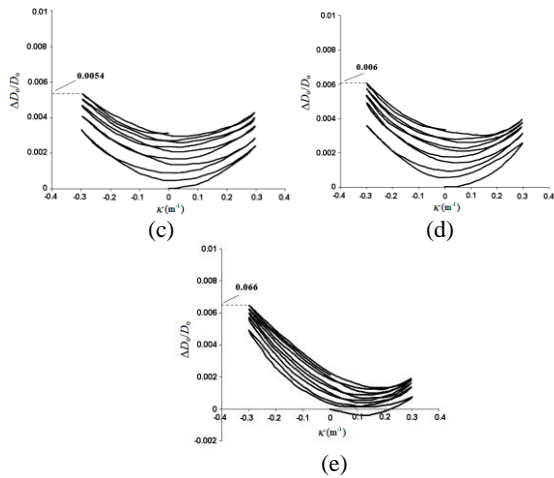
Lee et al.
The Response and Failure of Local Sharp-cut Circular Tubes with Different Diameter-to-thickness Ratios Submitted to
Cyclic Bending

(c)

(d)

(e)

Fig. 11 Experimental ovalization ($\Delta D_o/D_o$)-curvature (κ) curves for local sharp-cut 6061-T6 aluminum alloy tubes with $D_o/t = 31.0$ and $a =$ (a) 0.0, (b) 0.15, (c) 0.3, (d) 0.45 and (e) 0.6 mm under cyclic bending
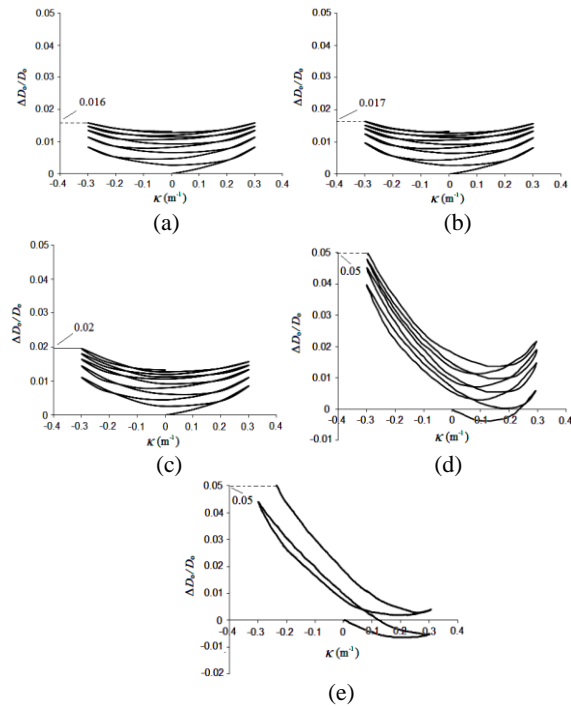

(a)

(b)

(c)

(d)

(e)

Fig. 12 Experimental ovalization ($\Delta D_o/D_o$) - curvature (κ) curves for local sharp-cut 6061-T6 aluminum alloy tubes with $D_o/t = 60.0$ and $a =$ (a) 0.0, (b) 0.075, (c) 0.15, (d) 0.225 and (e) 0.3 mm under cyclic bending

Failure

Figs. 13(a)-(c) present the experimental data of the cyclic controlled curvature (κ_c/κ_o) versus the number of bending cycles required to produce failure (N_f) for local-cut 6061-T6

aluminum alloy tubes with $D_o/t = 16.5$, 31.0 and 60.0, respectively, under cyclic bending. The controlled curvature was normalized by $\kappa_o = t/D_o^2$ [2]. For a certain κ_c/κ_o and a, tubes with a larger D_o/t ratios led to a lower N_f. In addition, for a certain D_o/t ratio and κ_c/κ_o, tubes with a larger a led to a lower N_f.
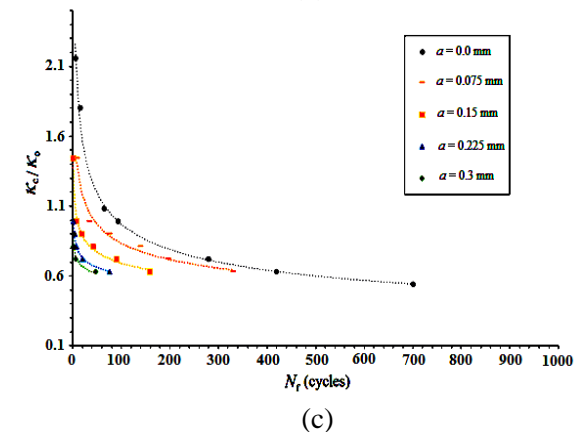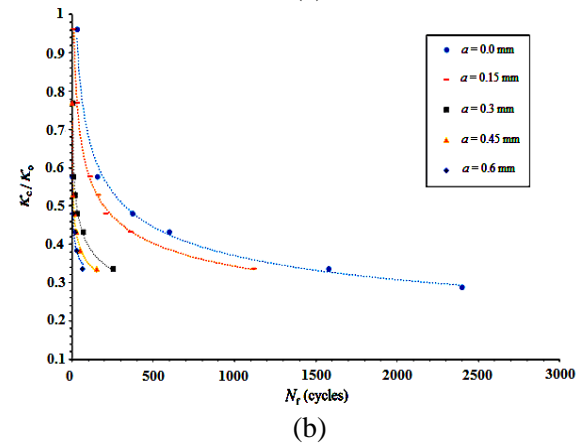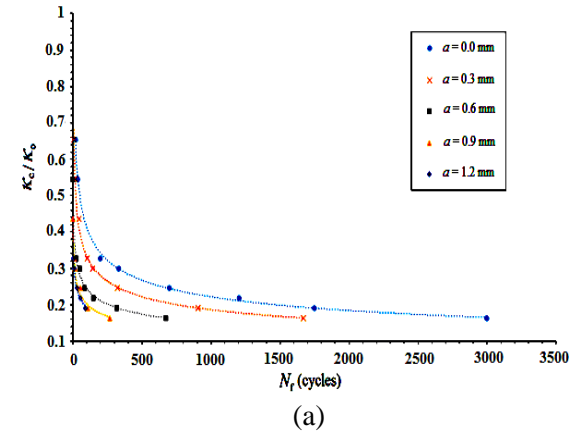

(a)

(b)

(c)

Fig. 13 Experimental controlled curvature (κ_c/κ_o) - number of bending cycles required to produce failure (N_f) curves for local sharp-cut 6061-T6 aluminum alloy tubes with $D_o/t =$ (a) 16.5, (b) 31.0 and (c) 60.0 under cyclic bending

Subsequently, the experimental data in Figs. 13(a)-(c) were plotted on a log-log scale, and five straight dot lines were observed in Figs. 14(a)-(c). Note that the dot lines were determined by the least square method. It can be seen that five unparallel dot lines corresponding to five different a for any D_o/t ratio.
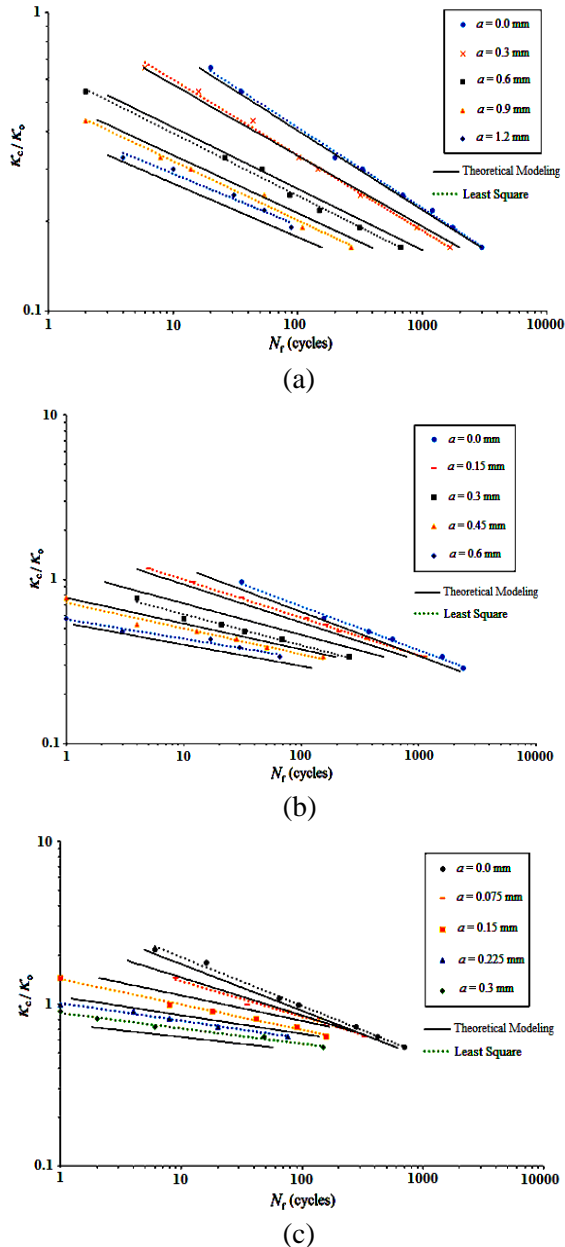

(a)

(b)

(c)

Fig. 14 Experimental and modeled controlled curvature (κ_c/κ_o) - number of bending cycles required to produce failure (N_f) curves for local sharp-cut 6061-T6 aluminum alloy tubes with D_o/t = (a) 16.5, (b) 31.0 and (c) 60.0 under cyclic bending on a log-log scale

In 1987, Kyriakides and Shaw [2] proposed an empirical formulation to describe the relationship between κ_c/κ_o and N_f to be:

$$\kappa_c/\kappa_o = C (N_f)^{-\alpha} \qquad (1)$$

or

$$\log \kappa_c/\kappa_o = \log C - \alpha \log N_f \qquad (2)$$

where C and α are the material parameters, which are related to the material and D_o/t ratios. The parameter C is the amount of κ_c/κ_o when $N_f = 1$, and the parameter α is the slope of the log-log plot. The formulation has been successfully simulated the κ_c/κ_o-N_f relationships for 6061-T6 aluminum alloy and 1018 carbon steel smooth tubes subjected to cyclic bending [2]. In this study, the liner relationships between ln$C$ and a/t and lnα and a/t were found in Figs. 15(a)-(c) and Fig. 16(a)-(c). Therefore, we write

$$\ln C = C_o - \beta (a/t) \qquad (3)$$

and

$$\ln \alpha = \alpha_o - \gamma (a/t) \qquad (4)$$

where C_o, β, α_o and γ are material parameters. Due to the linear relationship, the quantities of C_o and β were the intercepts and slopes in Figs. 15(a)-15(c) for D_o/t = 16.5, 31.0 and 60.0, respectively, and quantities of α_o and γ were the intercepts and slopes in Figs. 16(a)-16(c) for D_o/t = 16.5, 31.0 and 60.0, respectively. Table 3 show the magnitudes of C_o, β, α_o and γ for D_o/t = 16.5, 31.0 and 60.0.

Table 3 Magnitudes of C_o, β, α_o and γ for D_o/t = 16.5, 31.0 and 60.0

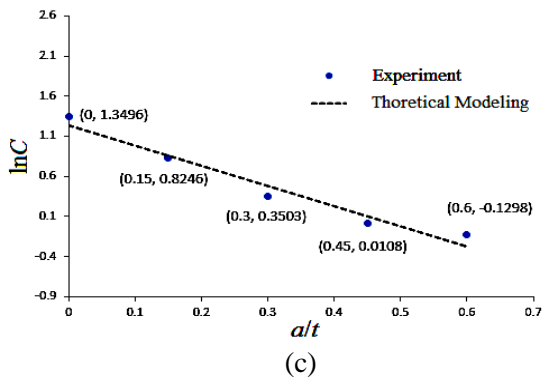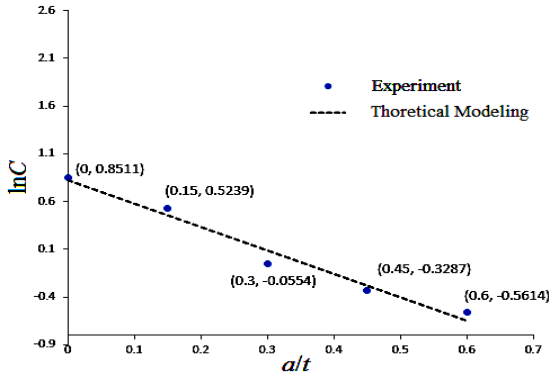| D_o/t	C_o	β	α_o	γ
16.5	0.356	2.083	-1.321	0.717
31.0	0.849	2.667	-1.332	1.167
60.0	1.258	2.495	-1.227	2.167

(a)

(b)

(c)
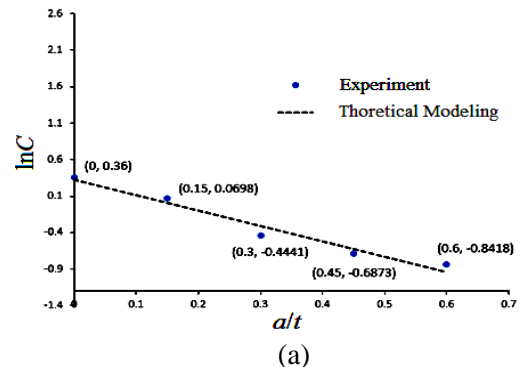
Fig. 15 The relationship between ln$C$ and a/t for D_o/t = (a) 16.5, (b) 31.0 and (c) 60
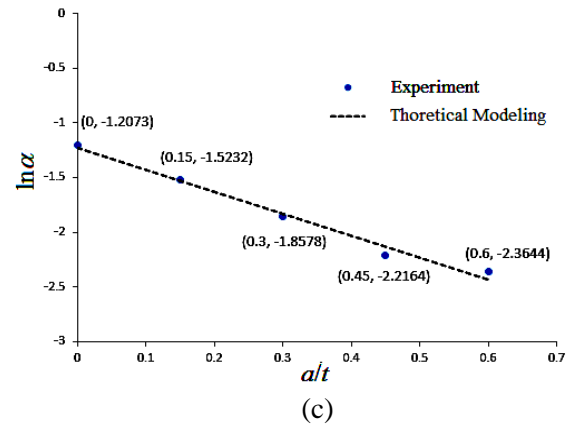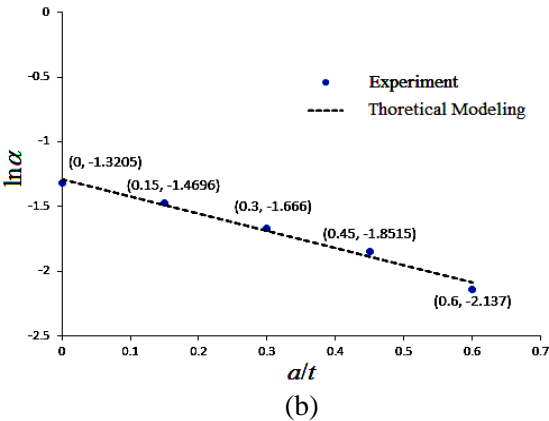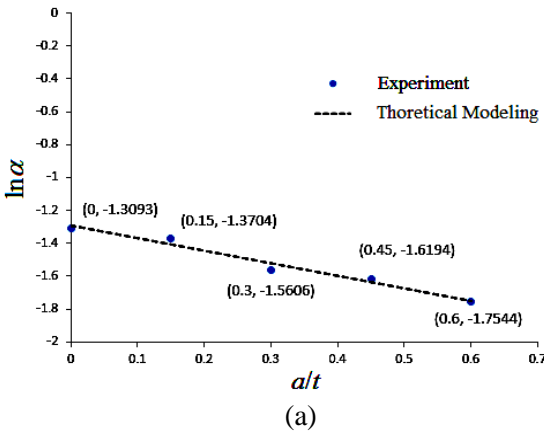

(a)

(b)

(c)

Fig. 16 The relationship between lnα and a/t for D_o/t = (a) 16.5, (b) 31.0 and (c) 60.0

Next, we assumed that the material parameters C_o, β, α_o and γ were related to the D_o/t ratios. In this study, we tried to find the linear relationships. After a lot of attempts, the linear relationships for C_o and D_o/t ratios, β and D_o/t ratios, α_o and D_o/t ratios, γ and D_o/t ratios were obtained in Figs. 17(a)-(d), respectively. Thus, the linear relationships were written as:

$$C_o^2 = a_1(D_o/t) + a_2 \tag{5}$$

$$\beta^2(D_o/t) = b_1(D_o/t) + b_2 \tag{6}$$

$$\alpha_o^2(D_o/t) = c_1(D_o/t) + c_2 \tag{7}$$

and

$$1/\gamma = d_1/(D_o/t) + d_2 \tag{8}$$

where a_1, a_2, b_1, b_2, c_1, c_2, d_1 and d_2 are material constants. The magnitudes of a_1 and a_2 were the slope and intercept in Fig 17(a), respectively, amounts of b_1 and b_2 were the slope and intercept in Fig 17(b), respectively, values of c_1 and c_2 were the slope and intercept in Fig 17(c), respectively, and magnitudes of d_1 and d_2 were

(a)
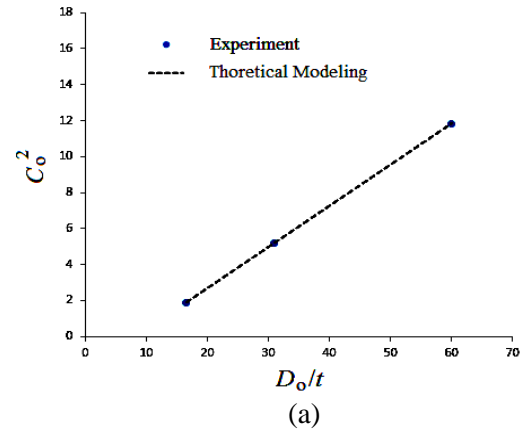
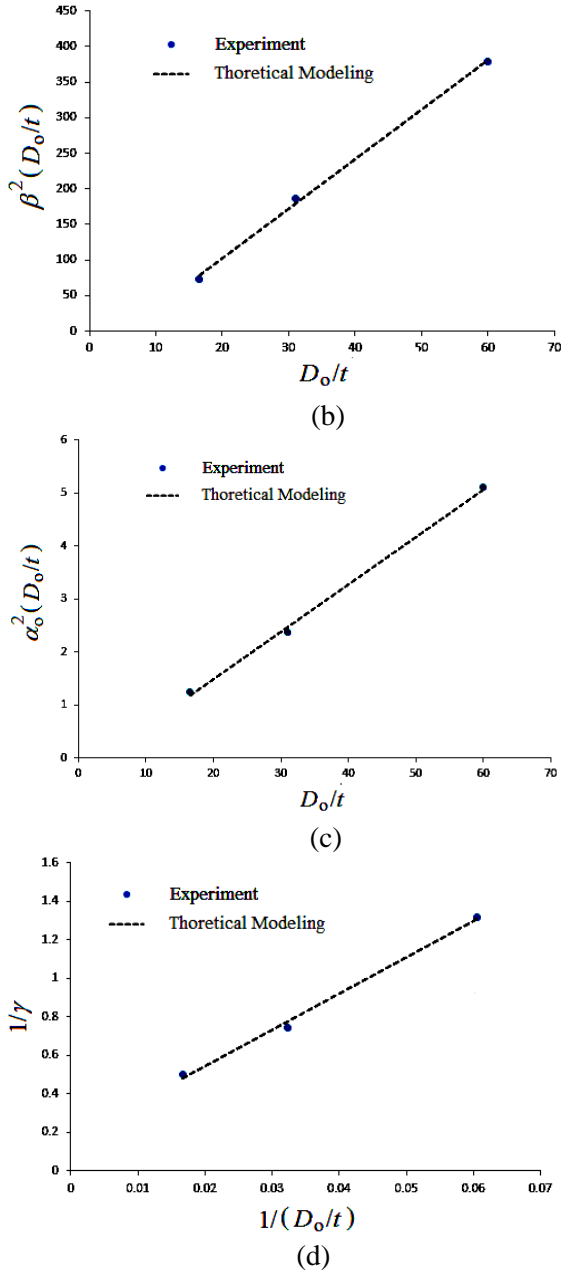Fig. 17 (a) The relationship between C_0^2 and D_o/t, (b) the relationship between $\beta^2(D_o/t)$ and D_o/t, (c) the relationship between $\alpha_o^2(D_o/t)$ and D_o/t, and (d) the relationship between $1/\gamma$ and $1/(D_o/t)$

the slope and intercept in Fig 17(d), respectively. These material constants were determined to be 0.228, -1.781, 7.011, -40.661, 0.089, -0.191, 0.021 and -0.062, respectively. In addition, Eqs. (5)-(8) are applicable in $16.5 \leq D_o/t \leq 60.0$.

Finally, Eqs. (2)-(8) and the material parameters had been obtained were used to simulate the experimental data in Figs. 14(a)-(c).

The modeled results of the relationship between the controlled curvature (κ_c/κ_o) and number of bending cycles required to produce failure (N_f) curves for local sharp-cut 6061-T6 aluminum alloy tubes with D_o/t = 16.5, 31.0 and 60.0, respectively, under cyclic bending on a log-log scale are depict in Figs. 14(a)-(c) in solid lines. Good agreement between the experimental and simulated results has been achieved.

V. CONCLUSIONS

This study investigated the response and failure of the local sharp-cut 6061-T6 aluminum alloy tubes with different D_o/t ratios submitted to cyclic bending. Some important conclusions are sorted as follows according to the experimental and simulated results:

(1) The experimental M-κ relationship for the local sharp-cut 6061-T6 aluminum alloy tubes with any a or D_o/t ratio displayed a closed hysteresis loop from the first bending cycle. Since the sharp cut was small and local, the cut depth had almost no influence on the M-κ curve for a certain D_o/t ratio.

(2) The experimental $\Delta D_o/D_o$-κ relationship for local sharp-cut 6061-T6 aluminum alloy tubes with any D_o/t ratio or a revealed an increasing and ratcheting trend with the number of bending cycles. The $\Delta D_o/D_o$-κ relationships were symmetrical for a = 0.0 mm, but asymmetrical for $a \neq 0.0$ mm. In addition, the tubes with a larger D_o/t or a led to more asymmetrical trend and a larger ovalization.

(3) The empirical formulation of Eq. (2) proposed by Kyriakides and Shaw [2] was modified to simulate the κ/κ_o-N_f relationship for the local sharp-cut 6061-T6 aluminum alloy tubes with different D_o/t ratios submitted to cyclic bending. According to the experimental data, the forms of the material parameters, C and α, were proposed in Eqs. (3) and (4), respectively. In addition, The forms of the material parameters, C_o, β, α_o and γ, were proposed in Eqs. (5)-(8), respectively. The results simulated by Eqs. (2)-(8) were in good agreement with the experimental findings (Figs. 14(a)-(c)).

V. REFERENCES

Lee et al.
The Response and Failure of Local Sharp-cut Circular Tubes with Different Diameter-to-thickness Ratios Submitted to
Cyclic Bending

[1] Shaw, P. K. and Kyriakides, S., "Inelastic Analysis of Thin-walled Tubes under Cyclic Bending," Int. J. Solids Struct., Vol. 21, No. 11, pp. 1073-1110, 1985.

[2] Kyriakides, S. and Shaw, P. K., "Inelastic Buckling of Tubes under Cyclic Loads," ASME J. Pre. Ves. Tech., Vol. 109, No. 2, pp. 169-178, 1987.

[3] Corona, E. and Kyriakides, S., "An Experimental Investigation of the Degradation and Buckling of Circular Tubes under Cyclic Bending and External Pressure," Thin-Walled Struct., Vol. 12, Is. 3, pp. 229-263, 1991.

[4] Vaze, S. and Corona, E., "Degradation and Collapse of Square Tubes under Cyclic Bending," Thin-Walled Struct., Vol. 31, No. 4, pp. 325-341, 1998.

[5] Corona, E. and Kyriakides, S., "Asymmetric Collapse Modes of Pipes under Combined Bending and Pressure," J. Eng. Mech., Vol. 126, No. 12, pp. 1232-1239, 2000.

[6] Corona, E., Lee, L. H. and Kyriakides, S., "Yield Anisotropic Effects on Buckling of Circular Tubes under Bending," Int. J. Solids Struct., Vol. 43, No. 22, pp. 7099-7118, 2006.

[7] Limam, A., Lee, L. H., Corana, E. and Kyriakides, S., "Inelastic Wrinkling and Collapse of Tubes under Combined Bending and Internal Pressure," Int. J. Mech. Sci., Vol. 52, Is. 5, pp. 637-647, 2010.

[8] Limam, A., Lee, L. H. and Kyriakides, S., "On the Collapse of Dented Tubes under Combined Bending and Internal Pressure," Int. J. Mech. Sci., Vol. 55, Is. 1, pp. 1-12, 2012.

[9] Bechle, N. J. and Kyriakides, S., "Localization of NiTi Tubes under Bending," Int. J. Solids Struct., Vol. 51, No. 5, pp. 967-980, 2014.

[10] Jiang, D., Kyriakides, S., Bechle, N. J. and Landis, C. M., "Bending of Pseudo Elastic NiTi Tubes," Int. J. Solids Struct., Vol. 124, pp. 192-214, 2017.

[11] Yuan, W. and Mirmiran, A., "Buckling Analysis of Concrete-filled FRP Tubes," Int. J. Struct. Stab. Dyn., Vol. 1, No. 3, pp. 367-383, 2001.

[12] Elchalakani, M., Zhao, X. L. and Grzebieta, R. H., "Plastic Mechanism Analysis of Circular Tubes under Pure Bending," Int. J. Mech. Sci., Vol. 44, No. 6, 1117-1143, 2002.

[13] Jiao, H. and Zhao, X. L., "Section Slenderness Limits of Very High Strength Circular Steel Tubes in Bending," Thin-Walled Struct., Vol. 42, No. 9, pp. 1257-1271, 2004.

[14] Houliara, S. and Karamanos, S. A., "Buckling and Post-buckling of Long Pressurized Elastic Thin-walled Tubes under In-plane Bending," Int. J. Nonlinear Mech., Vol. 41, No. 4, pp. 491- 511, 2006.

[15] Elchalakani, M., Zhao, X. L. and Grzebieta, R. H., "Variable Amplitude Cyclic Pure Bending Tests to Determine Fully Ductile Section Slenderness Limits for Cold-formed CHS," Eng. Struct., Vol. 28, No. 9, pp. 1223-1235, 2006.

[16] Yazdani, H. and Nayebi, A., "Continuum Damage Mechanics Analysis of Thin-walled Tube under Cyclic Bending and Internal Constant Pressure," Int. J. Appl. Mech., Vol. 5, No. 4, 1350038 [20 pages], 2013.

[17] Fan, H. G., Chen, Z. P., Feng, W. Z., Zhou, F. and Cao, G. W., "Dynamic Buckling of Cylindrical Shells with Arbitrary Axisymmetric Thickness Vibration under Time Dependent External Pressure," Int. J. Struct. Stab. Dyn., Vol. 15, No. 3, 1450053 [21 pages], 2015.

[18] Elchalakani, M., Karrech, A. and Hassanein, M. F. and Yang, B., "Plastic and Yield Slenderness Limits for Circular Concrete Filled Tubes Subjected to Static Pure Bending," Thin-Walled Struct., Vol. 109, pp. 50-64, 2016.

[19] Shamass, R., Alfano, G. and Guarracino, F., "On Elastoplastic Buckling Analysis of Cylinders under Nonproportional Loading by Differential Quadrature Method," Int. J. Struct. Stab. Dyn., Vol. 17, No. 7, 1750072 [40 pages], 2017.

[20] Pan, W. F., Wang, T. R. and Hsu, C. M., "A Curvature-Ovalization Measurement Apparatus for Circular Tubes under Cyclic Bending," Exp. Mech., Vol. 38, No. 2, pp.

99-102, 1998.

[21] Pan, W. F. and Fan, C. H., "An Experimental Study on the Effect of Curvature-rate at Preloading Stage on Subsequent Creep or Relaxation of Thin-walled Tubes under Pure Bending," JSME Int. J., Ser. A, Vol. 41, No. 4, pp. 525-531, 1998.

[22] Pan, W. F. and Her, Y. S., "Viscoplastic Collapse of Thin-walled Tubes under Cyclic Bending," ASME J. Eng. Mat. Tech., Vol. 120, No. 4, pp. 287-290, 1998.

[23] Lee, K. L., Pan, W. F. and Kuo, J. N., "The Influence of the Diameter-to-thickness Ratio on the Stability of Circular Tubes under Cyclic Bending," Int. J. Solids Struct., Vol. 38, No. 14, pp. 2401-2413, 2001.

[24] Lee, K. L., Pan, W. F. and Hsu, C. M., "Experimental and Theoretical Evaluations of the Effect between Diameter-to-thickness Ratio and Curvature-rate on the Stability of Circular Tubes under Cyclic Bending," JSME Int. J., Ser. A, Vol. 47, No. 2, pp. 212-222, 2004.

[25] Chang, K. H., Pan, W. F. and Lee, K. L., "Mean Moment Effect of Thin-walled Tubes under Cyclic Bending," Struct. Eng. Mech., Vol. 28, No. 5, pp. 495-514, 2008.

[26] Chang, K. H. and Pan, W. F., "Buckling Life Estimation of Circular Tubes under Cyclic Bending," Int. J. Solids Struct., Vol. 46, No. 2, pp. 254-270, 2009.

[27] Lee, K. L., Hung, C. Y. and Pan, W. F., "Variation of Ovalization for Sharp-notched Circular Tubes under Cyclic Bending," J. Mech., Vol. 26, No. 3, pp. 403 -411, 2010.

[28] Lee, K. L., "Mechanical Behavior and Buckling Failure of Sharp-notched Circular Tubes under Cyclic Bending," Struct. Eng. Mech., Vol. 34, No. 3, pp. 367 -376, 2010.

[29] 洪兆宇、李國龍和潘文峰，"不同尖銳凹槽深度 304 不銹鋼管在循環彎曲負載下黏塑性行為之實驗分析"，技術學刊，第 26 卷，第 4 期，235-242 頁，2011。

[30] Lee, K. L., Hsu, C. M. and Pan, W. F., "Viscoplastic Collapse of Sharp-notched Circular Tubes under Cyclic Bending," Acta Mech. Solida Sinica, Vol. 22, No. 6, pp. 629-641, 2013.

[31] Lee, K. L., Hsu, C. M. and Pan, W. F., "Response of Sharp-notched Circular Tubes under Bending Creep and Relaxation," Mech. Eng. J., Vol. 1, No. 2, pp. 1-14, 2014.

[32] Chang, K. H , Lee, K. L. and Pan, W. F., "Buckling Failure of 310 Stainless Steel Tubes with Different Diameter-to-thickness Ratios under Cyclic Bending," Steel Comp. Struct., Vol. 10, No. 3, pp. 224-245, 2010.

[33] Lee, K. L., Hsu, C. M. and Pan, W. F., "The Influence of the Diameter-to-thickness Ratio on the Response and Collapse of Sharp-notched Circular Tubes under Cyclic Bending," J. Mech., Vol. 28, No. 3, pp. 461-468, 2012.

[34] Lee, K. L., Chern, R. T. and Pan, W. F., "The Response of 6061-T6 Aluminum Alloy Tubes with Different Chop Depths under Cyclic Bending," J. Chung Cheng Inst. Tech., Vol. 45, No. 1, pp. 19-29, 2016.

Lee et al.
The Response and Failure of Local Sharp-cut Circular Tubes with Different Diameter-to-thickness Ratios Submitted to Cyclic Bending